J1 CrIS Radiometric Calibration

Dave Tobin, Hank Revercomb, Joe Taylor, Bob Knuteson, Dan DeSlover, Lori Borg, Graeme Martin
Space Science and Engineering Center, University of Wisconsin-Madison

2015 JPSS Science Teams Annual Meeting
Session 6c: ATMS/CrIS Breakout
NOAA Center for Weather and Climate Prediction, College Park, MD
26 August 2015

Outline

- Radiometric Calibration Equations
  - In-orbit and TVAC
- Diagnostic Mode data analysis
  - Out-of-band signal analysis, including nonlinearity
- ECT view data analysis
  - Linear calibrations
  - ECT view temperature analysis
  - Nonlinearity determinations
- Radiometric Uncertainty (RU) estimates
  - ICT parameter uncertainties
  - Nonlinearity uncertainty
  - RU for TVAC ECT view data
  - Example RU for In-orbit sky view
- Polarization Effects
  - Theory and impact on Calibration
  - S-NPP CrIS/VIIRS comparison examples
- Summary and Future Work

Acknowledgements

- Lawrence Suwinski, Rebecca Malloy, Steve Wells … of Exelis/Harris
- Joe Predina, Logistikos
- Mark Esplin, SDL
- Dave Johnson, NASA
- Yong Han, NOAA

Radiometric Calibration Equations*

TVAC: $N_{ECT} = Re\{(C'_{ECT} - C'_{ST}) / (C'_{ICT} - C'_{ST})\} (R_{ICT} - R_{ST}) + R_{ST}$

On-Orbit: $N_{Earth} = Re\{(C'_{Earth} - C'_{SP}) / (C'_{ICT} - C'_{SP})\} R_{ICT}$

with:

ECT: External Calibration Target

ST: Space Target

ICT: Internal Calibration Target

SP: Deep Space view

Complex spectra: C = FFT(Interferogram)

Nonlinearity Corrections: $C' = C \cdot (1 + 2\, a_2\, V_{DC})$

Predicted ICT view Radiances: $R_{ICT} = B(T_{ICT}) - r_{spec}\,[R_{specBG} - B(T_{ICT})] - r_{diff}\,[R_{diffBG} - B(T_{ICT})]$

Predicted ST view Radiances: $R_{ST} = \varepsilon_{ST}\, B(T_{ST}) + (1-\varepsilon_{ST})\, B(T_{ICT})$

*** Not addressing spectral calibration and/or spectral ringing impacts on calibration in this presentation.**

Diagnostic Mode Data

Example FOV9 ICT view spectra, Mission Nominal TVAC

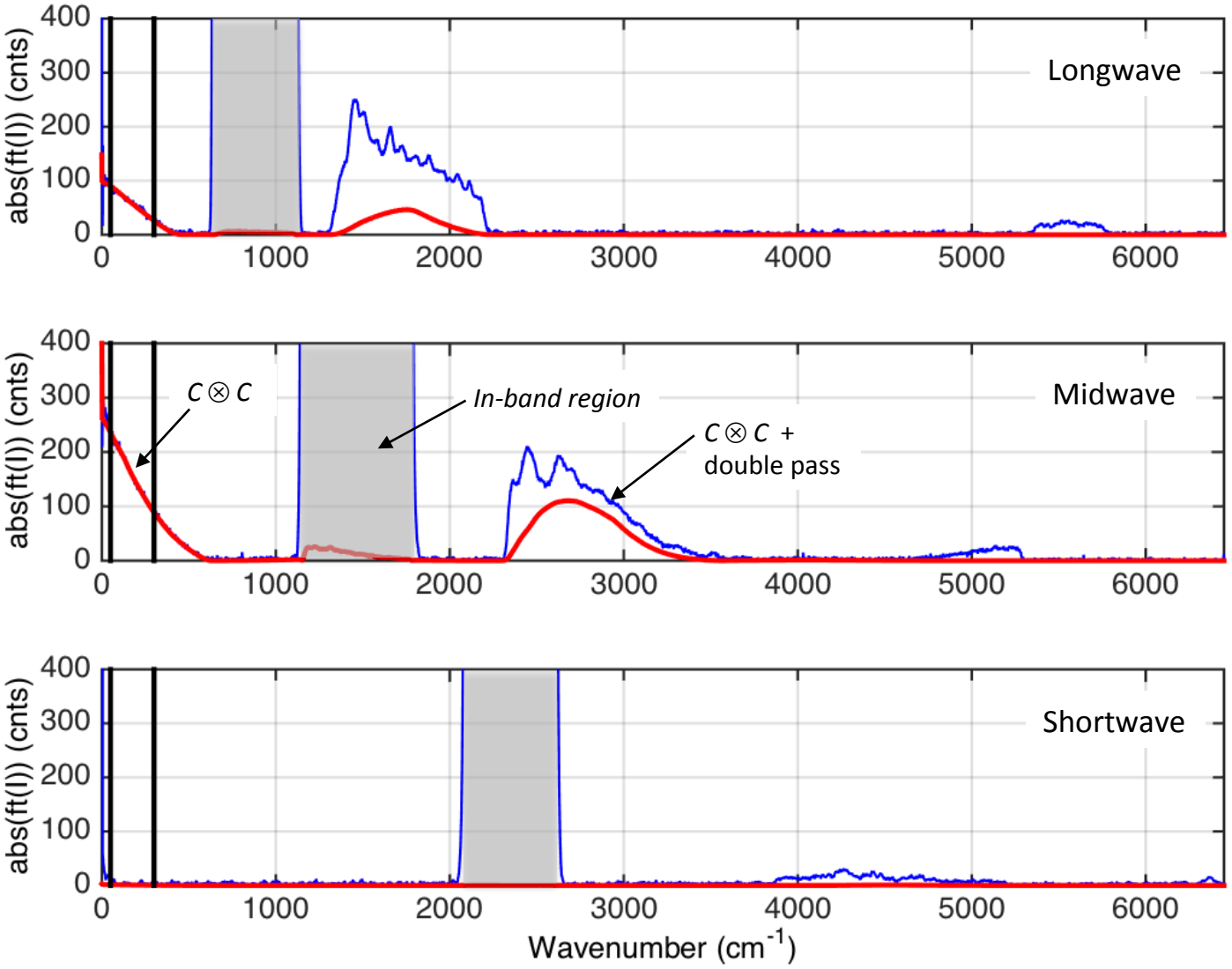

C_{ICT}

$a_2 \bullet C_{ICT} \otimes C_{ICT}$

Diagnostic Mode Data

quadratic nonlinearity coefficients, a_2, from various DM datasets

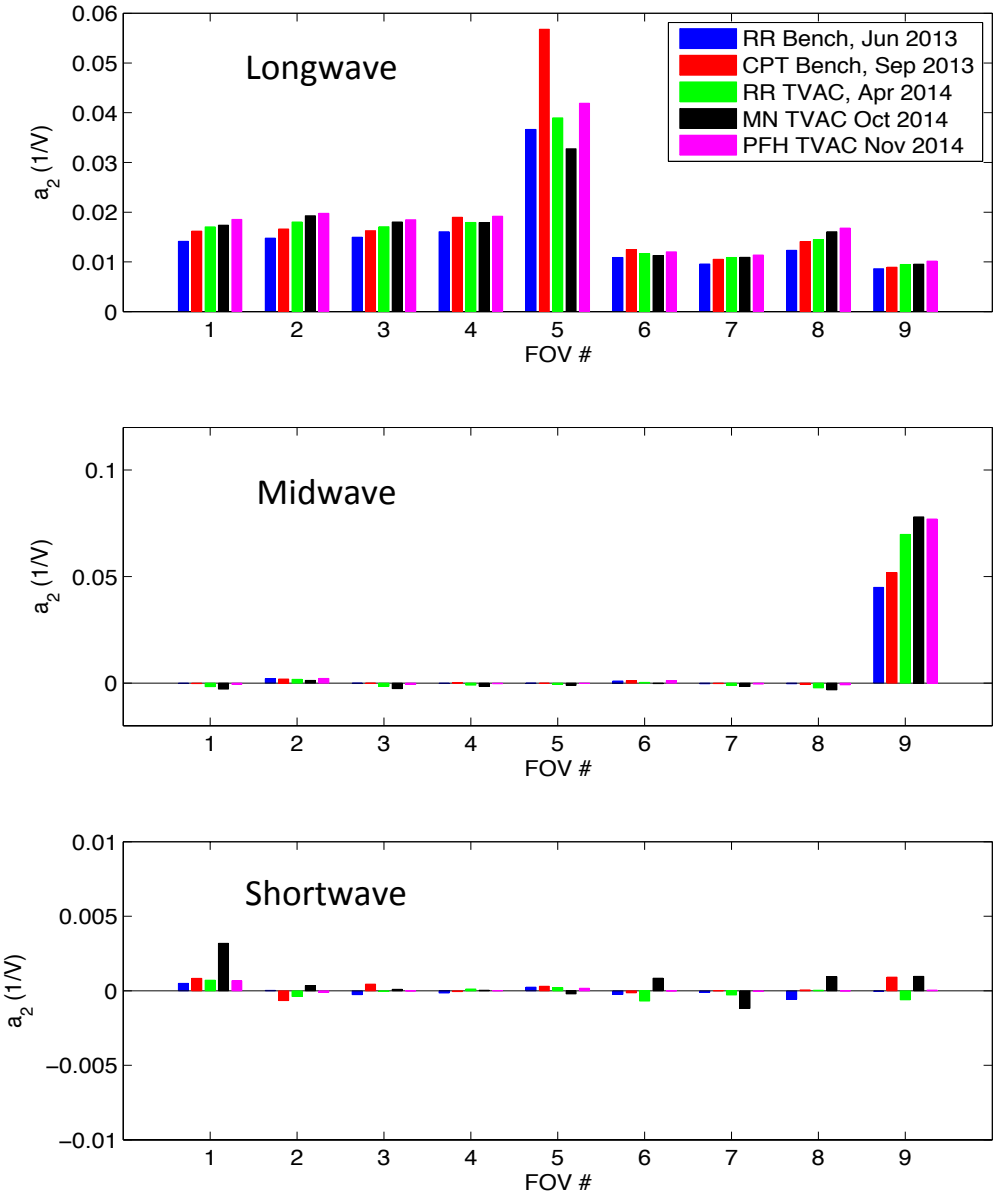

$a_2 = -Re\{ C/C \otimes C \}$
for 50-300 cm^{-1}

Diagnostic Mode Data, Key Findings:

- Out-of-band signals in the DM data show quadratic nonlinearity behavior. There are no obvious signs of higher order nonlinearities.
- These values are in good agreement with similar analyses performed by Exelis.
- All FOVs in the longwave band show significant levels of nonlinearity. With the exception of FOV5, all longwave FOVs have roughly the same level of quadratic nonlinearity (of roughly the same level of magnitude as S-NPP longwave FOVs). FOV5 is roughly twice as nonlinear as the other longwave FOVs.
- With the exception of FOV9, the midwave FOVs show very low levels of nonlinearity. The FOV9 a_2 value is roughly half that of the most non-linear midwave FOV (FOV7) on S-NPP.
- While small, all five of the a_2 values for midwave FOV2 are positive, suggesting there may be a small amount of nonlinearity. This requires further investigation.
- All shortwave FOVs show very small a_2 values. Further work is required to assess if there is a very low level of nonlinearity indicated in these results.
- Some larger differences are noted between the different tests. Further analysis is needed to determine if these are indicative of real changes in nonlinearity or due to other uncertainties in the results.

ECT view data analysis, Radiometric Nonlinearity Determination:

- Normal Mode ECT view data collected for six set-point temperatures
- FOV dependent ECT temperatures derived from linear SW and linear MW CrIS observations
- Quadratic Nonlinearity coefficients, a_2, determined by minimizing ECT view residuals

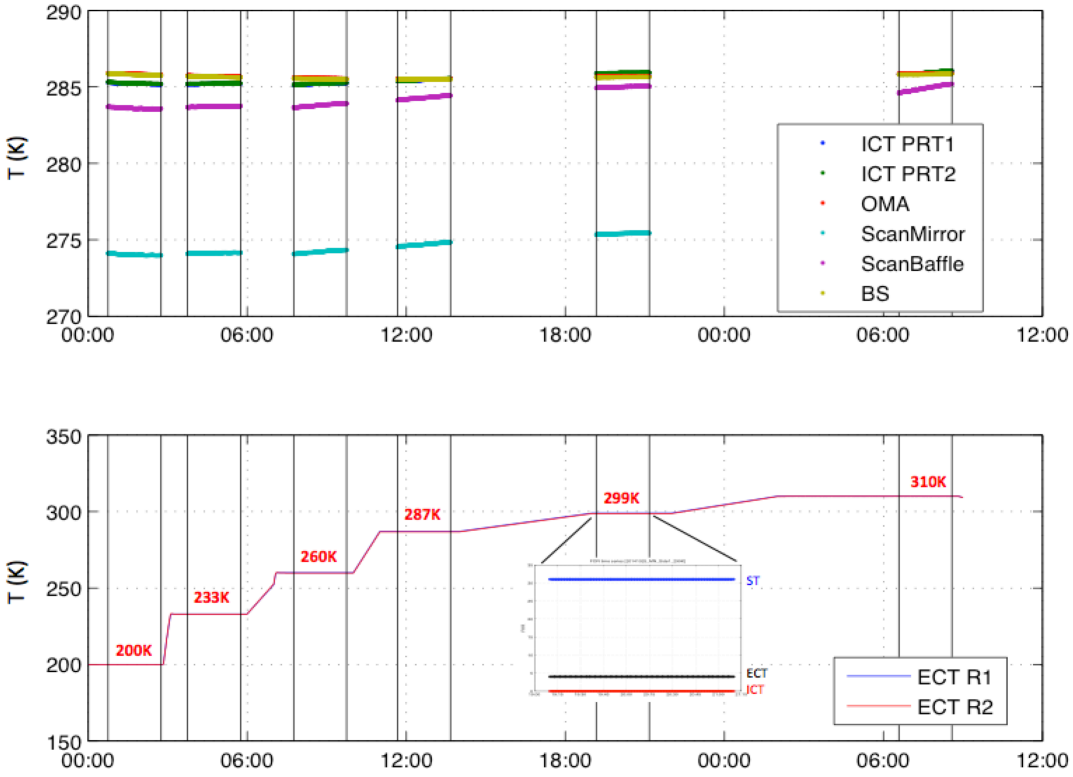

Timeline of Mission Nominal Side 1 ECT view data collected on 25-26 October 2014

ECT view data analysis,
ECT view residuals for linear calibrations

ECT view residuals,
$N_{ECT} - R_{ECT}$, *with*

$R_{ECT} = \varepsilon_{ECT} \bullet B(T_{ECT}) + \ldots$
$(1 - \varepsilon_{ECT}) \bullet B(T_{ICT})$

$R_{ST} = e_{ST} \bullet B(T_{ST}) + \ldots$
$(1 - e_{ST}) \bullet B(T_{ICT})$

T_{ECT} = mean of backplate R1, R2 measurements

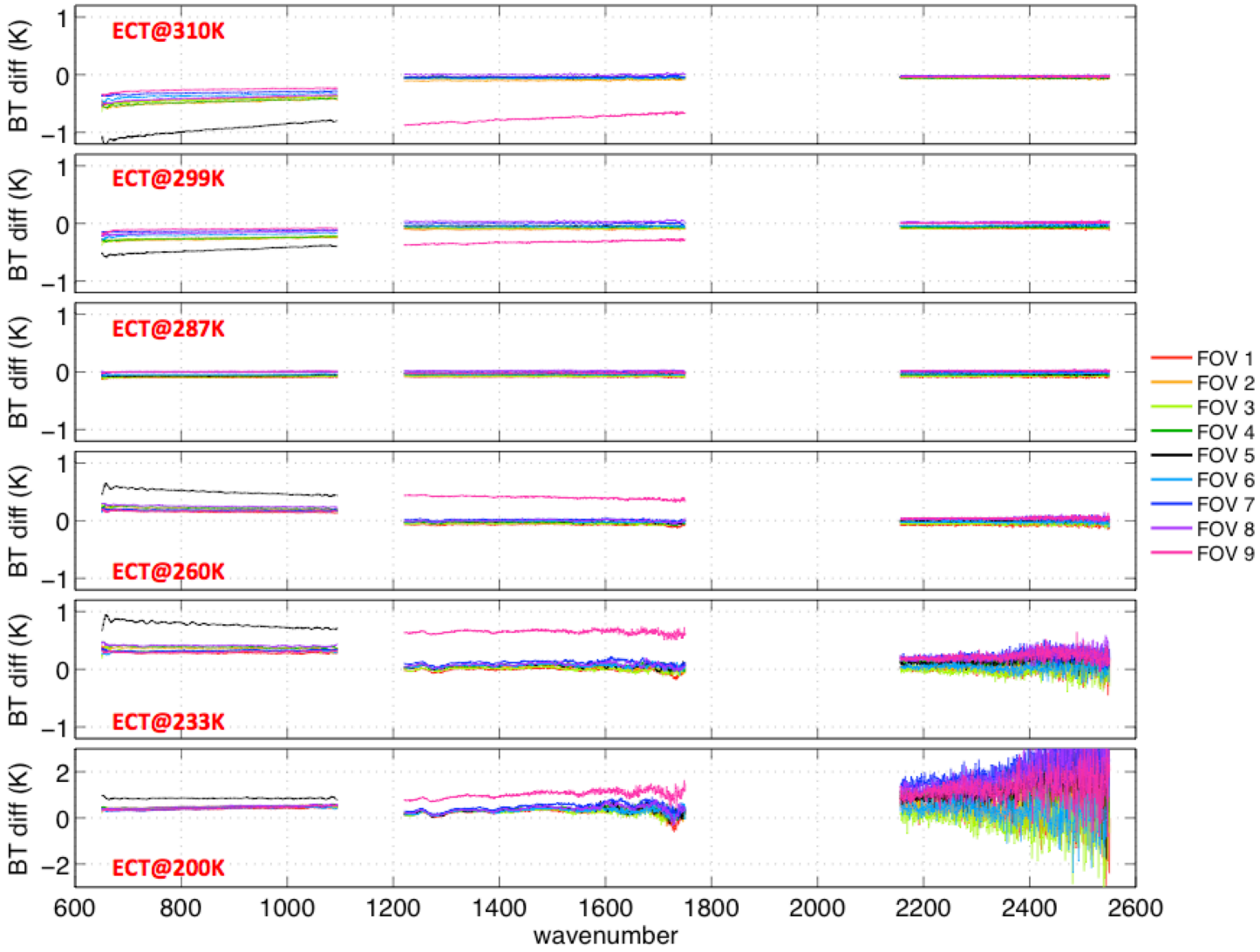

ECT view residuals for linear calibrations. Key observations:

1) The shortwave band spectra show negligible nonlinearity signals, with the residuals largely independent of ECT temperature,

2) Shortwave band residuals display a FOV pattern consistent with a vertical temperature gradient on the backplate of the ECT,

3) Residuals for the 287K set-point, where TECT ~ TICT, do not show spectral features correlated with the ICT emissivity, providing confidence in the knowledge of the ICT predicted radiances.

4) The longwave and midwave band residuals display noticeable nonlinear behavior for midwave FOV9 and all of the longwave FOVs, with negative residuals for the 310K and 299K setpoints above the ICT calibration temperature and positive residuals for the 260K, 233K, and 200K setpoints below the ICT calibration temperature,

5) The size of the nonlinearity signals are generally consistent with nonlinearity information from Diagnostic Mode data analysis, with midwave FOVs 1-8 displaying negligible nonlinearity, midwave FOV9 displaying large nonlinearity, and all longwave band FOVs displaying similar levels of nonlinearity but with FOV5 larger by about a factor of 2.

6) ECT residuals in the shortwave band for 233 and 200K show non-Plankian behavior consistent with uncertainties in the reflected component of the ECT and ST predicted radiances and also higher scatter in brightness temperature due to noise.

ECT view data analysis, example ECT temperatures from linear SW FOV spectra

310 K
<R1,R2>-<T_{FOV}> = 45 mK
max(T_{FOV})-min(T_{FOV}) = 38 mK

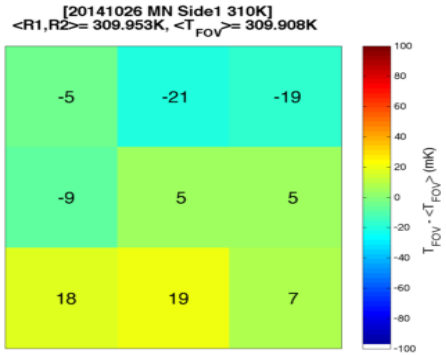

299 K
<R1,R2>-<T_{FOV}> = 43 mK
max(T_{FOV})-min(T_{FOV}) = 105 mK

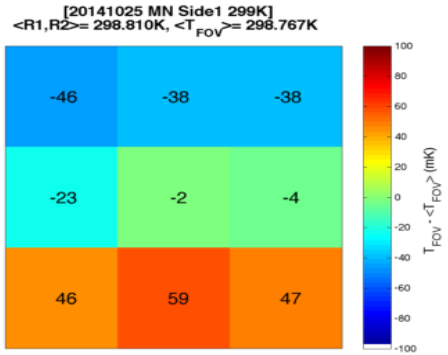

287 K
<R1,R2>-<T_{FOV}> = 34 mK
max(T_{FOV})-min(T_{FOV}) = 108 mK

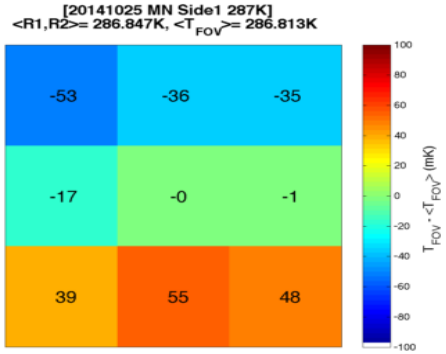

260 K
<R1,R2>-<T_{FOV}> = 15 mK
max(T_{FOV})-min(T_{FOV}) = 110 mK

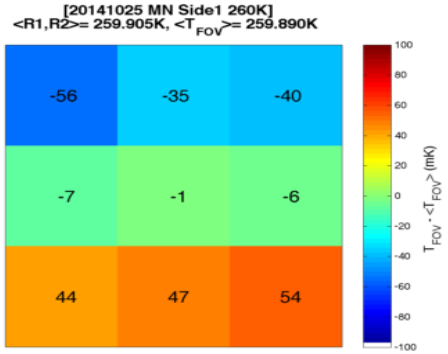

233 K
<R1,R2>-<T_{FOV}> = -99 mK
max(T_{FOV})-min(T_{FOV}) = 237 mK

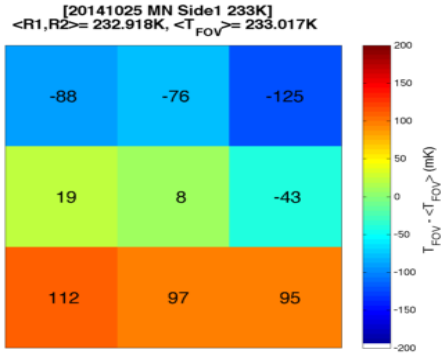

200 K
<R1,R2>-<T_{FOV}> = 0.8 K
max(T_{FOV})-min(T_{FOV}) = 1.6 K

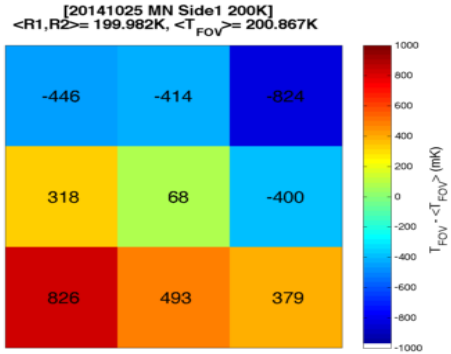

ECT view data analysis,
ECT view residuals for linear calibrations

ECT view residuals,
$N_{ECT} - R_{ECT}$, *with*

$R_{ECT} = \varepsilon_{ECT} \bullet B(T_{ECT}) + \ldots$
$(1 - \varepsilon_{ECT}) \bullet B(T_{ICT})$

$R_{ST} = e_{ST} \bullet B(T_{ST}) + \ldots$
$(1 - e_{ST}) \bullet B(T_{ICT})$

T_{ECT} = FOV dependent values determined from calibrated spectra for linear SW and MW FOVs

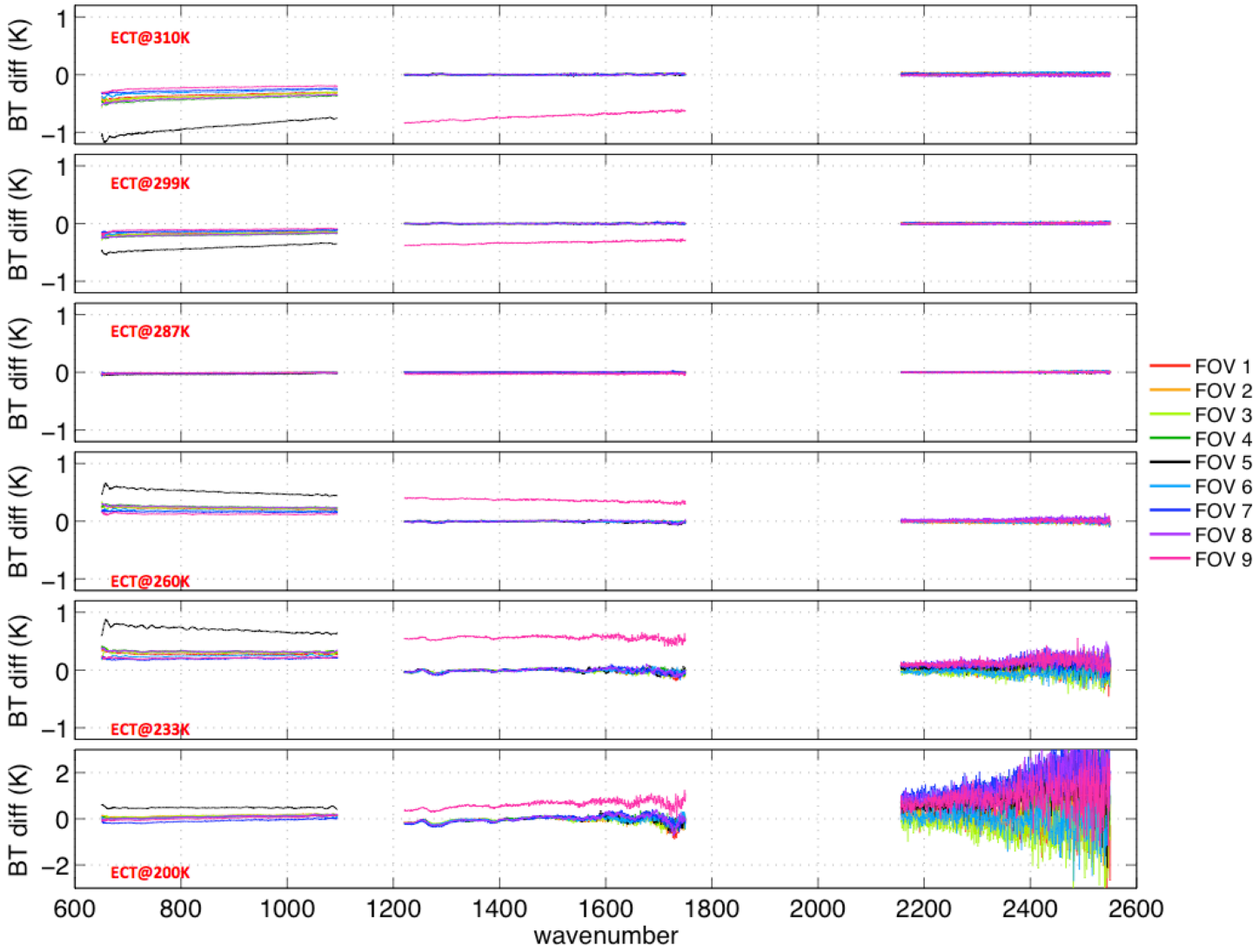

ECT view data analysis, ECT view residuals, with optimized a_2 values

ECT view residuals, $N_{ECT} - R_{ECT}$, *with*

$R_{ECT} = \varepsilon_{ECT} \bullet B(T_{ECT}) + \ldots$
$(1 - \varepsilon_{ECT}) \bullet B(T_{ICT})$

$R_{ST} = e_{ST} \bullet B(T_{ST}) + \ldots$
$(1 - e_{ST}) \bullet B(T_{ICT})$

T_{ECT} = FOV dependent values determined from calibrated spectra for linear SW and MW FOVs

a_2 values determined to minimize the 310K, 299K, and 260K residuals.

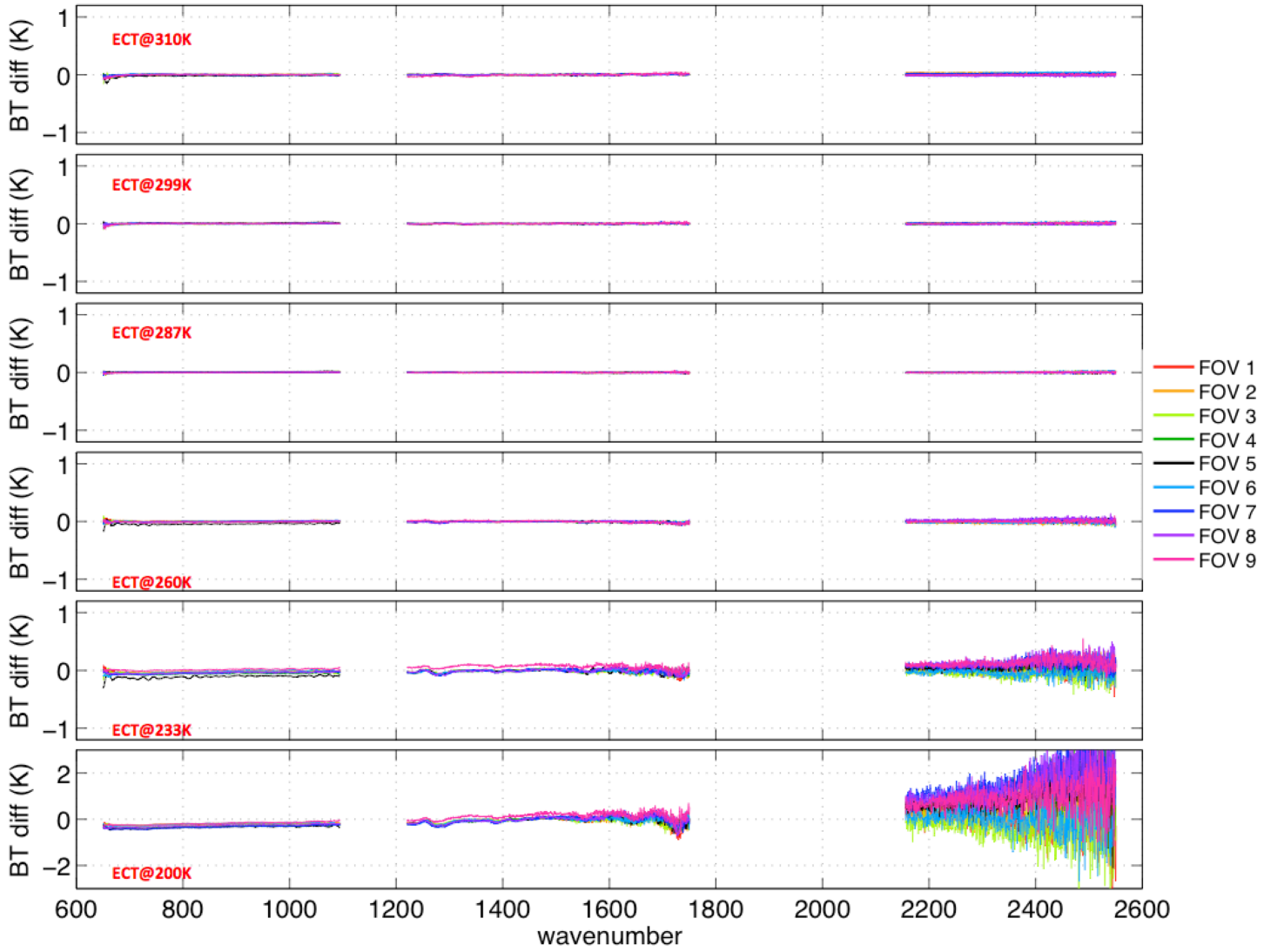

ECT view data analysis, ECT view residuals, with optimized a_2 values

ECT view residuals, $N_{ECT} - R_{ECT}$, *with*

$R_{ECT} = \varepsilon_{ECT} \bullet B(T_{ECT}) + \ldots$
$(1 - \varepsilon_{ECT}) \bullet B(T_{ICT})$

$R_{ST} = e_{ST} \bullet B(T_{ST}) + \ldots$
$(1 - e_{ST}) \bullet B(T_{ICT})$

T_{ECT} = FOV dependent values determined from calibrated spectra for linear SW and MW FOVs

a_2 values determined to minimize the 310K, 299K, and 260K residuals.

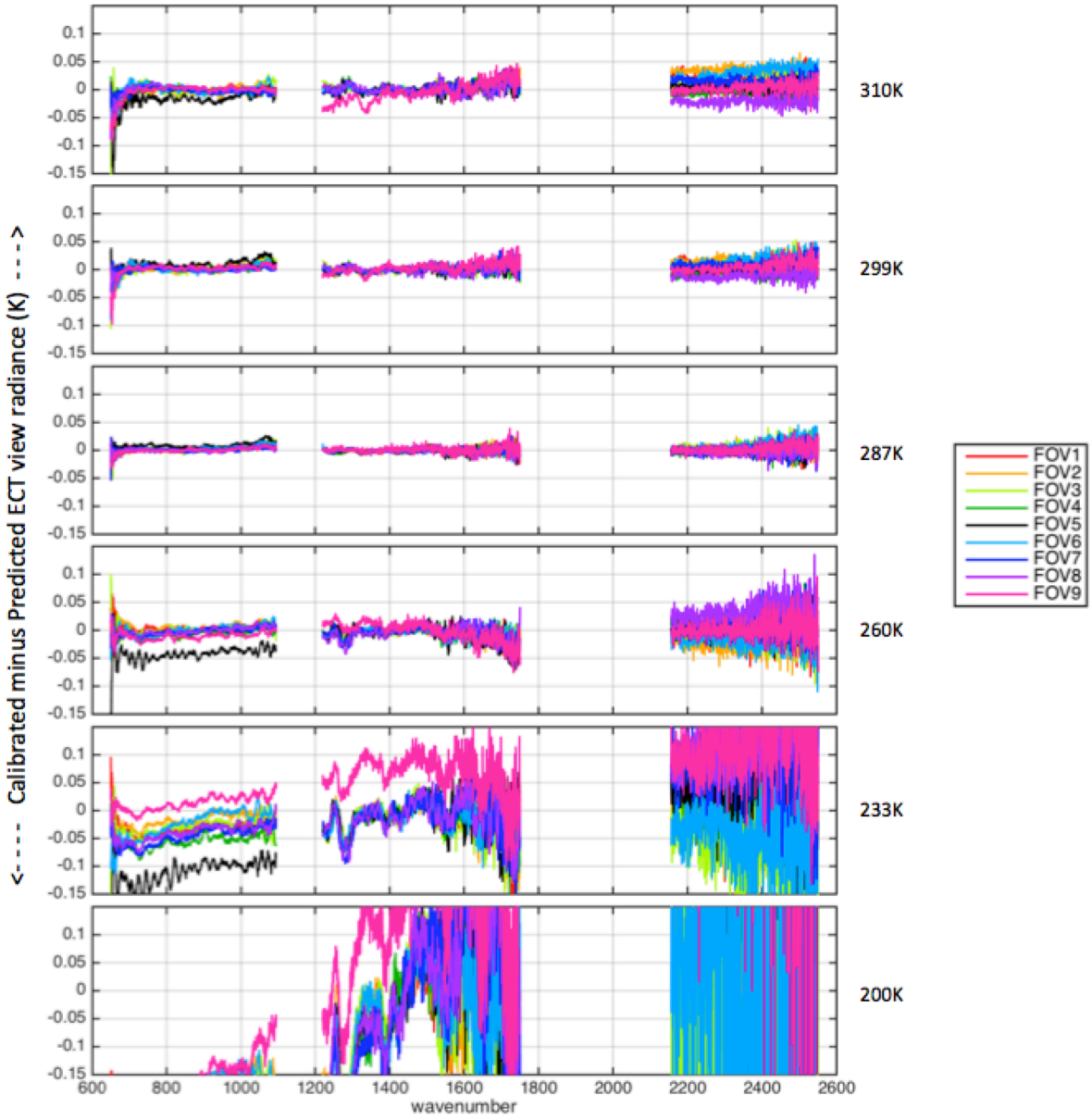

J1 Quadratic Nonlinearity coefficients from stepped ECT data, and comparison to S-NPP

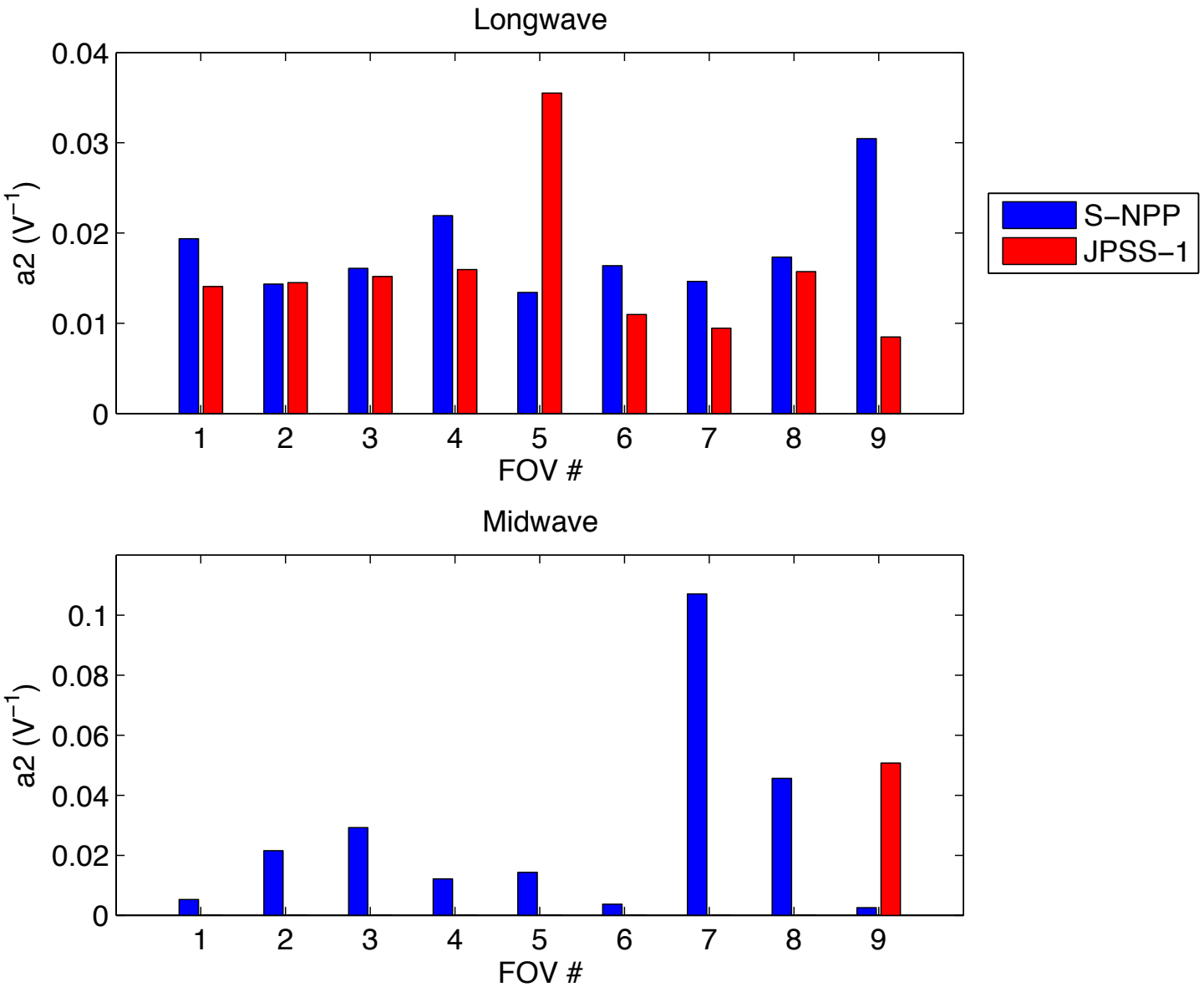

ECT view residuals and Nonlinearity Determination. Summary:

1) Temperature gradients of ~0.1K exist on the backplate of the ECT, and there are significant uncertainties in the absolute calibration of the ECT backplate R1 and R2 temperature sensors.

2) Using calibrated CrIS spectra for linear FOVs, this analysis relies on the absolute calibration of the CrIS ICT to determine the FOV dependent ECT temperatures for the various ECT set-points. Pending results of NIST TXR measurements of the ECT, we may re-do this analysis using new ECT temperatures. We endorse the efforts for a new ECT.

3) Quadratic nonlinearity coefficients are optimized/determined to reduce ECT residuals at 310K, 299K, and 260K, and resulting residuals are 50 mK or less. Residuals for 233K and 200K are larger and not used in the optimization due to larger uncertainties at these temperatures associated with the ECT and ST emissivities and temperatures.

4) J1 nonlinearity is qualitatively similar to S-NPP nonlinearity, with all LW FOVs showing appreciable nonlinearity and some very linear MW FOVs.

5) These J1 a2 values are included in the current Engineering Packet for initial on-orbit calibrations, and during the early Cal/Val phase the a2 values will be fine tuned to create optimal consistency of the radiometric calibration of LW and MW Earth view spectra (same approach as was used for S-NPP).

J1 Pre-Launch ECT view
Radiometric Uncertainty (RU) Estimates

Perturbation of the TVAC Calibration Equation:

$$N_{ECT} = Re\{(C'_{ECT} - C'_{ST}) / (C'_{ICT} - C'_{ST})\} (R_{ICT} - R_{ST}) + R_{ST}$$

Nonlinearity Corrections: $C' = C \cdot (1 + 2\, a_2\, V_{DC})$

Predicted ICT view Radiances: $R_{ICT} = B(T_{ICT})$ (ignoring small reflected contributions)

Predicted ST view Radiances: $R_{ST} = \varepsilon_{ST}\, B(T_{ST}) + (1-\varepsilon_{ST})\, B(T_{ICT})$

Predicted ECT view Radiances:

$$R_{ECT} = \varepsilon_{ECT}\, B(T_{ECT}) + (1-\varepsilon_{ECT})\, B(T_{ICT})$$

Parameter Uncertainties:

N_{ECT} parameter	Nominal Value	3-sigma Unc.
LW a_2	0.01 – 0.03 V^{-1}	25%
MW a_2	0, 0.05 V^{-1}	25%
T_{ICT}	287 K	0.114 K
ε_{ST}	0.9995	0.0009
T_{ST}	104 K	6 K
$T_{ST,\ Refll}$	287 K	9 K

R_{ECT} parameter	Nominal Value	3-sigma Unc.
ε_{ECT}	0.9995	0.0009
T_{ECT}	200 – 310K	0.2 K
$T_{ECT,Refl}$	287 K	15 K

J1 Radiometric Uncertainty (RU) Estimates: Predicted ICT radiance.

Predicted ICT view radiance for the specular 3-bounce trap design includes an emissive term and reflected terms due to the specular and diffuse reflections of the ICT:

$$R_{ICT} = B(T_{ICT}) - r_{spec}\,[R_{specBG} - B(T_{ICT})] - r_{diff}\,[R_{diffBG} - B(T_{ICT})]$$

The specular reflection term is computed as reflection from the beamsplitter and is estimated as $\frac{1}{2}\, r_{spec}\, B(T_{ICT})$. r_{spec} is ~0.03% and the specular reflection term is approximately 10 mK in BT with an uncertainty of 5 to 10 mK.

For the diffuse term, r_{diff} is very small and the diffuse emitting surfaces have temperature very close to T_{ICT}. This results in this diffuse reflection term being very small, on the order ~5 mK with uncertainty of 5 to 10 mK.

For the emissive term $B(T_{ICT})$, T_{ICT} has an uncertainty of 114 mK, significantly larger than the reflected term contributions and uncertainties. (A large fraction of the TICT uncertainty is due to the thermal gradient from the PRT sensor location to the ICT emitting surfaces).

For the following RU estimates, uncertainties in predicted ICT radiances include T_{ICT} contributions only and uncertainties in the reflected terms are ignored.

J1 Pre-Launch Nonlinearity Uncertainty

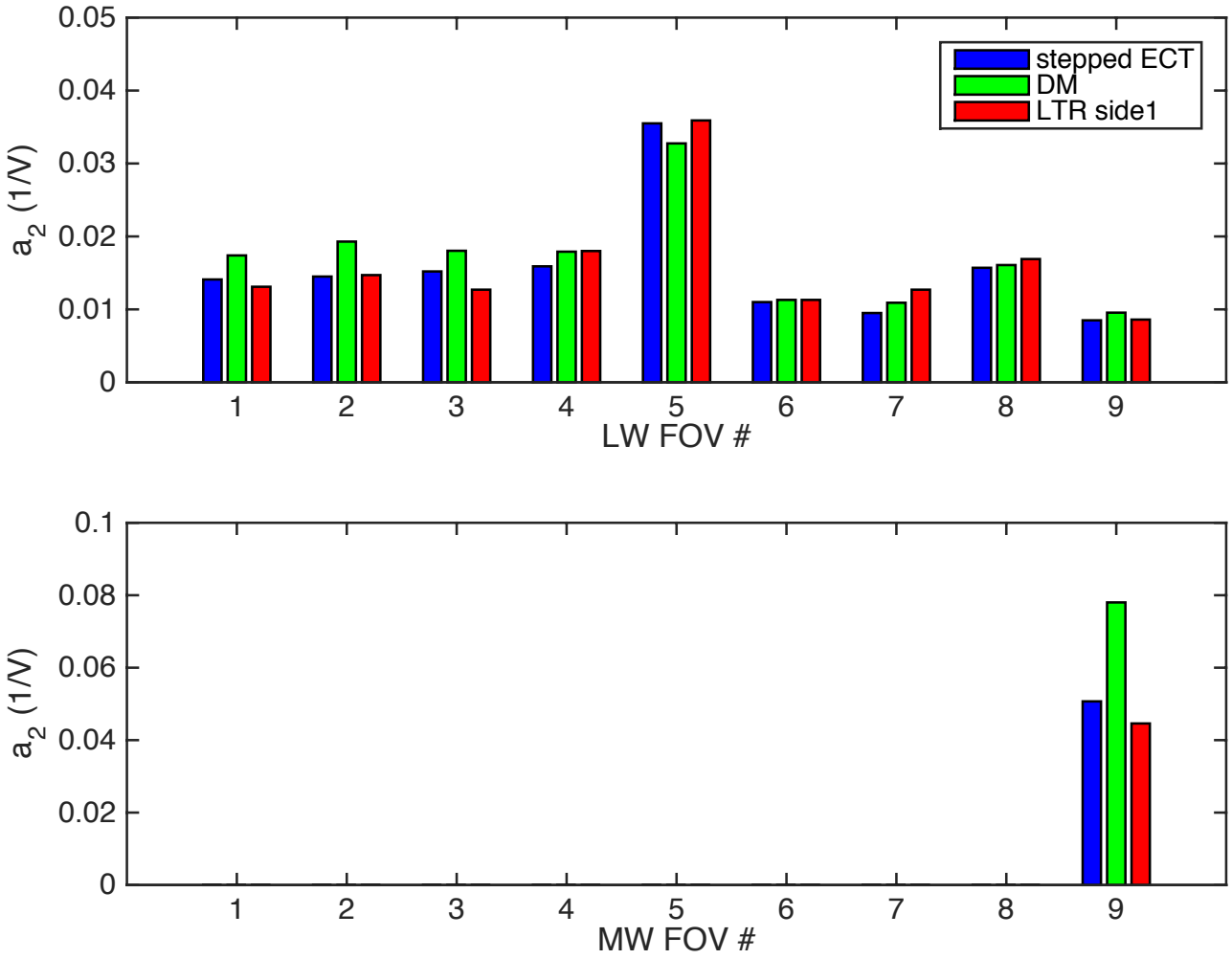

Comparison of quadratic nonlinearity coefficients from three pre-launch test data analysis methods: Stepped ECT view NM data, Diagnostic Mode harmonics, Long term repeatability c/o Mark Esplin.

J1 Pre-Launch ECT view
Radiometric Uncertainty (RU) Estimates

CrIS RU

- FOV 1
- FOV 2
- FOV 3
- FOV 4
- FOV 5
- FOV 6
- FOV 7
- FOV 8
- FOV 9

R_{ECT} Uncertainty

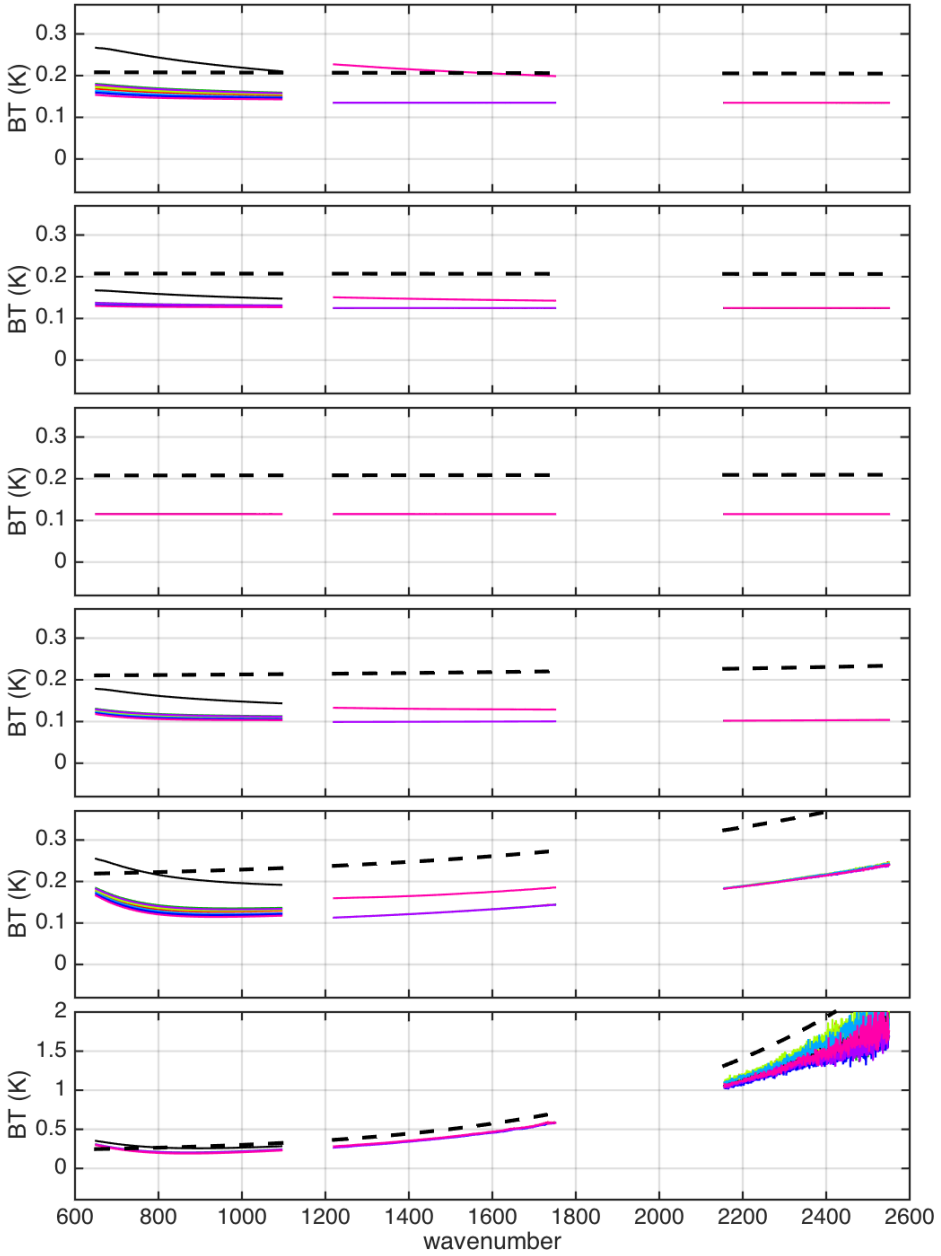

310 K

299 K

287 K

260 K

233 K

200 K

J1 Pre-Launch Earth view Radiometric Uncertainty (RU) Estimates

Perturbation of the in-orbit Calibration Equation using S-NPP Earth view data

$$N_{Earth} = Re\{(C'_{Earth} - C'_{SP}) / (C'_{ICT} - C'_{SP})\} R_{ICT}$$

Nonlinearity Corrections: $C' = C \cdot (1 + 2\, a_2\, V_{DC})$

Predicted ICT view Radiances: $R_{ICT} = B(T_{ICT})$ (ignoring small reflected contributions)

Parameter Uncertainties:

N_{Earth} parameter	Nominal Value	3-sigma Unc.
LW a_2	0.01 – 0.03 V^{-1}	25%
MW a_2	0, 0.05 V^{-1}	25%
T_{ICT}	287 K	0.114 K

J1 Pre-Launch Earth view RU Estimates

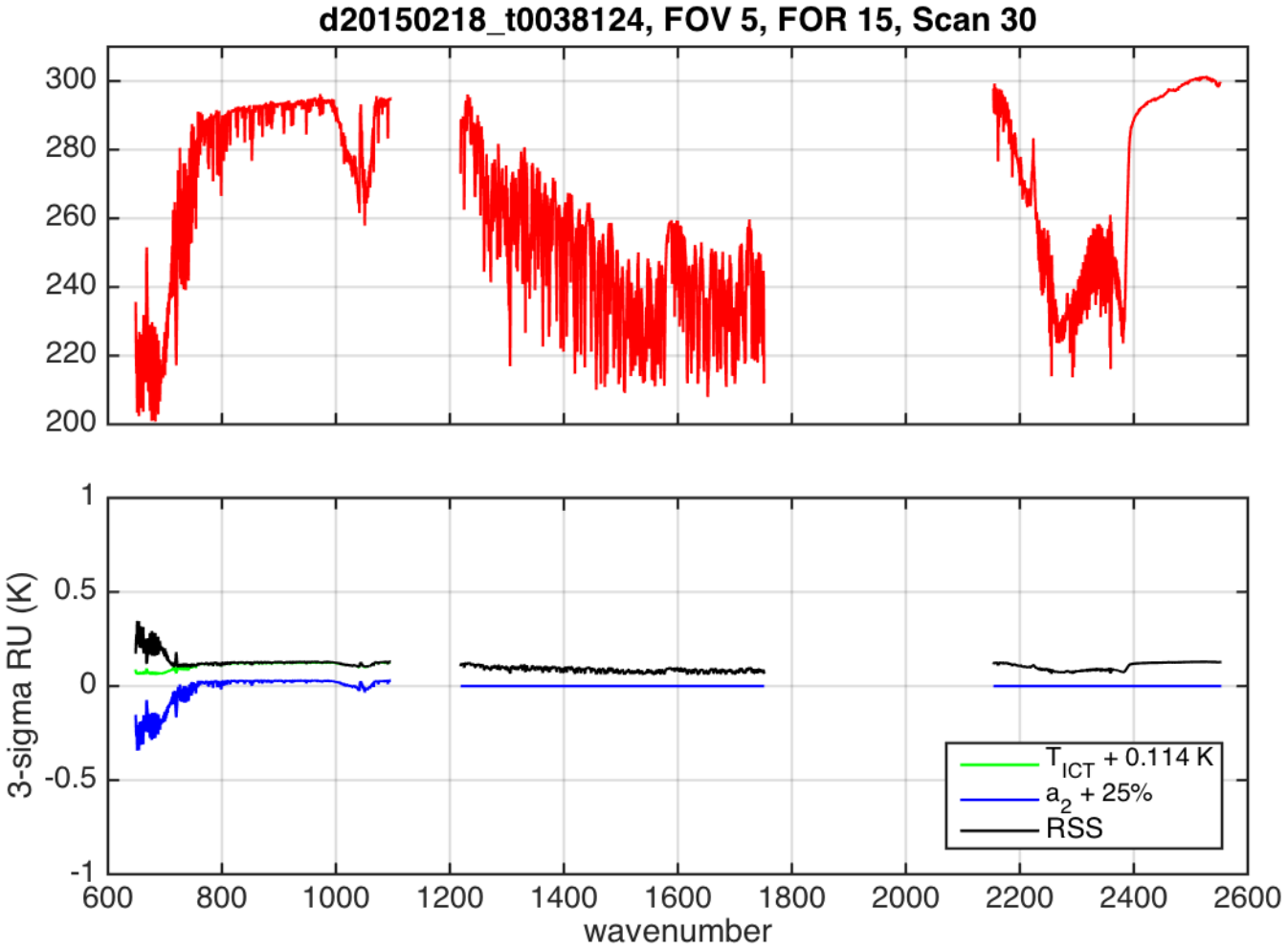

J1 Pre-Launch Earth view RU Estimates

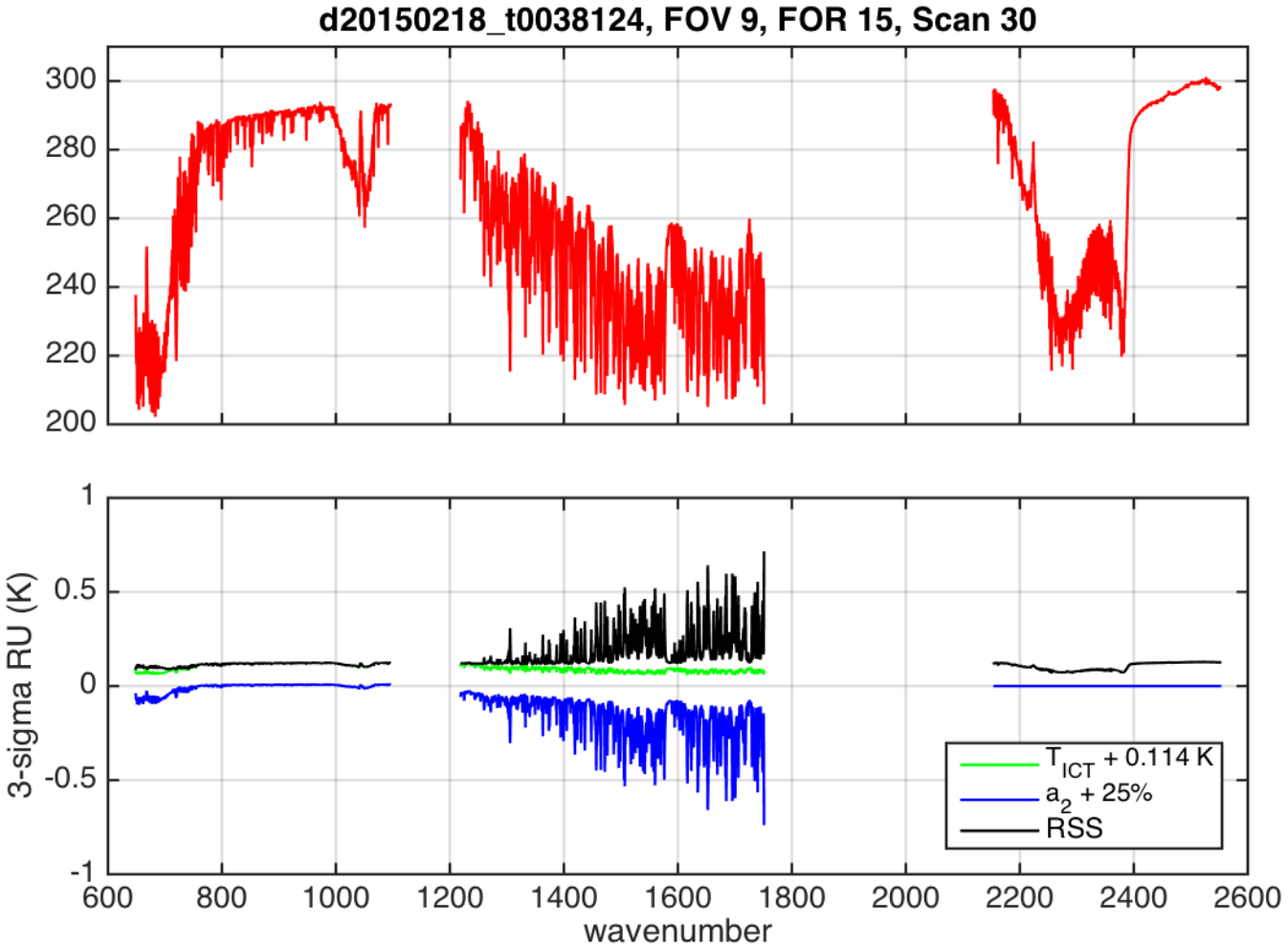

J1 Pre-Launch Earth view RU Estimates

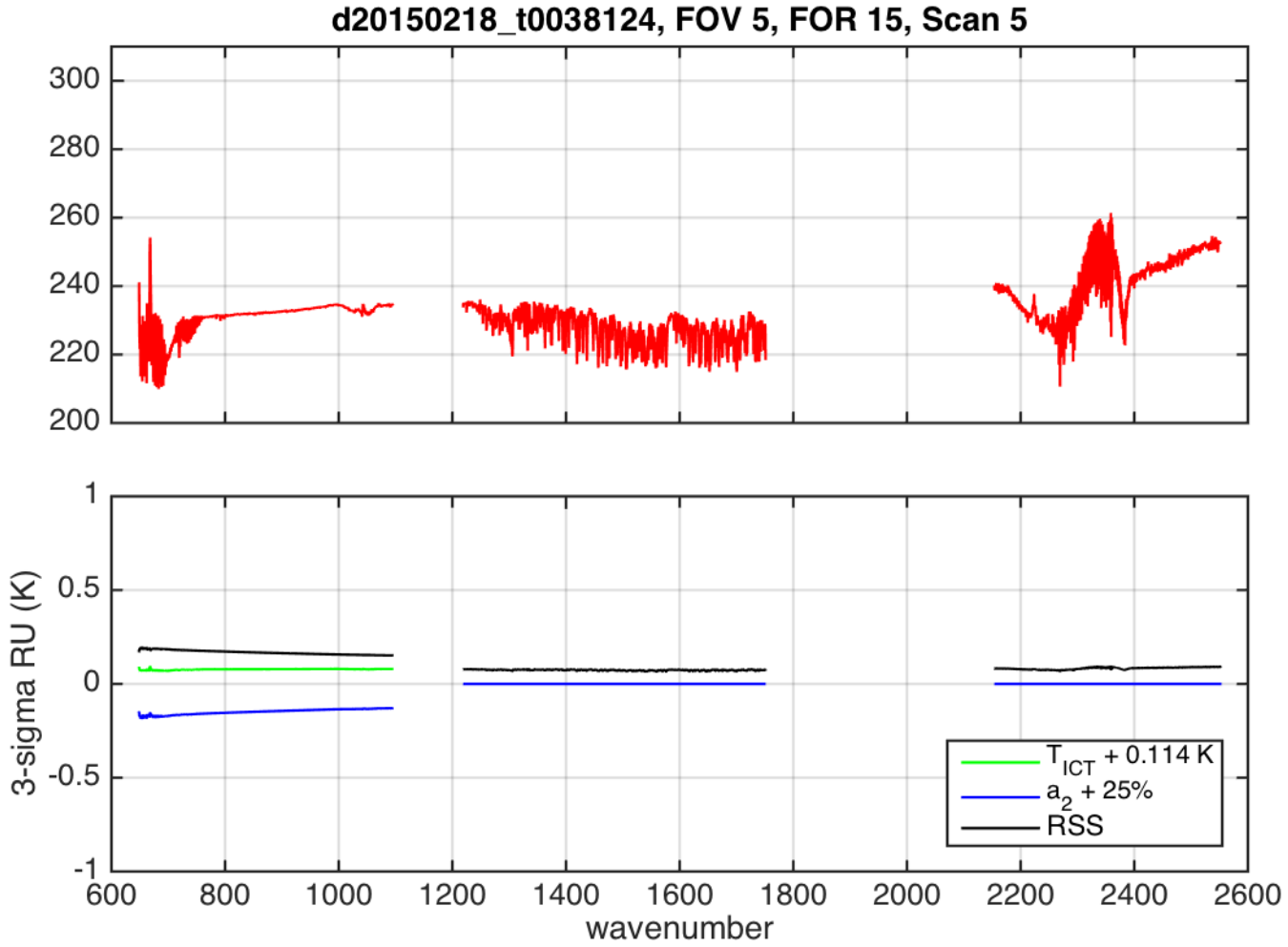

J1 Pre-Launch Earth view RU Estimates

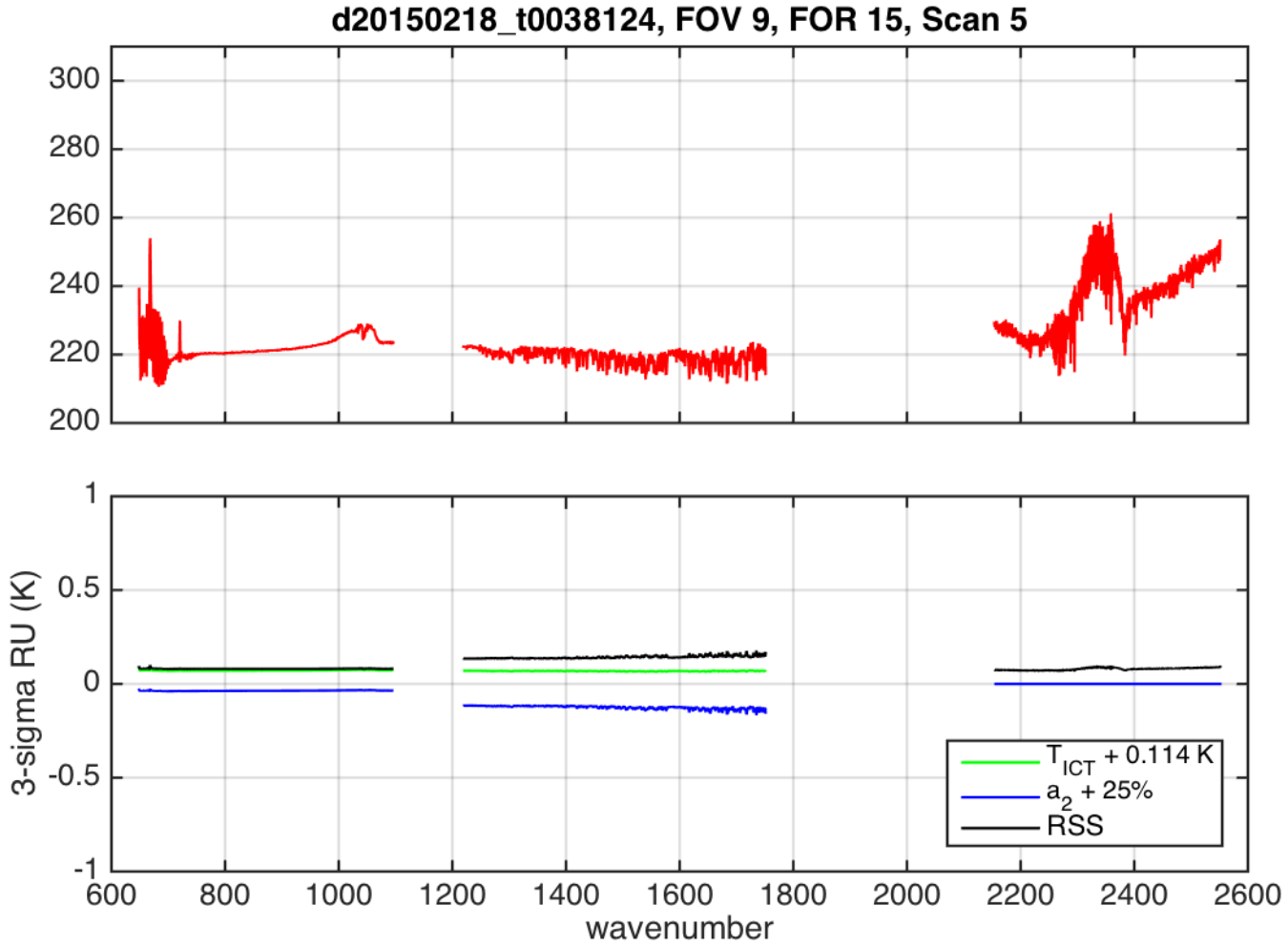

J1 Pre-Launch Earth view RU Estimates

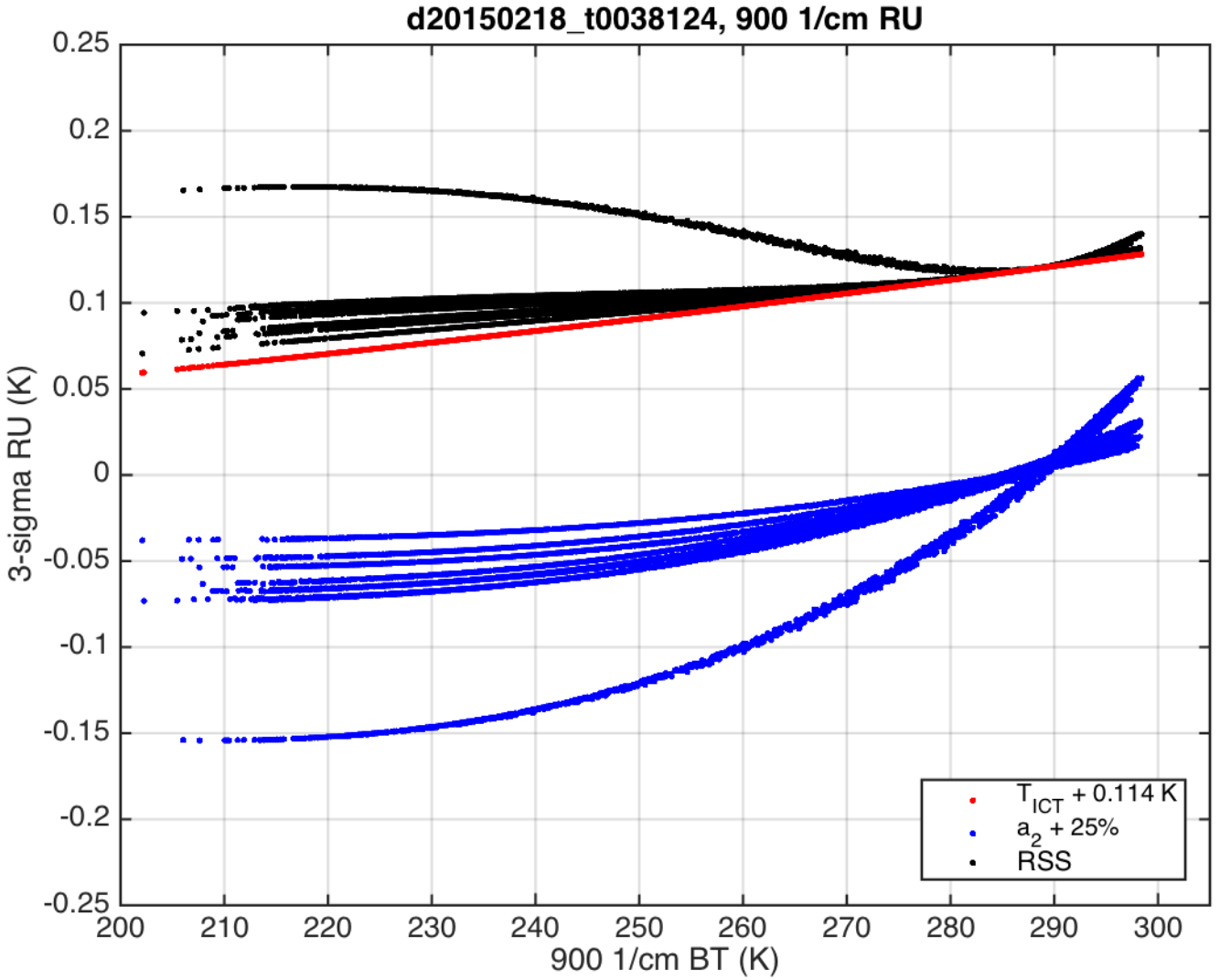

J1 Pre-launch RU summary

- **Pre-launch RU estimates for J1 CrIS are very similar to S-NPP estimates, and are dominated by ICT temperature and nonlinearity contributions.**
  - **ICT temperature uncertainty for J1 is very similar to S-NPP.**
  - **J1 CrIS has negligible contributions from ICT reflected terms due to the improved ICT design and implementation.**
  - **8 of the 9 MW FOVs are very linear on J1, whereas only MW FOVs 6 and 9 are linear on S-NPP. LW nonlinearity magnitude on J1 is very similar to S-NPP.**
  - **Pre-launch J1 nonlinearity coefficient uncertainty is approximately a factor of 2 lower than that of S-NPP.**
- **Nonlinearity coefficient tuning using Earth view data will reduce the MW FOV9 uncertainty to very small levels (using linear MW FOVs as reference), and LW nonlinearity consistency among FOVs will be optimized.**
- **Opposed to Exelis/Harris RU estimates, these RU estimates do not yet include contributions due to polarization, cross-talk, or other smaller contributions.**

CrIS Calibration Bias due to Polarization. Introduction:

- Incident radiance is partially polarized by reflection from the scene select mirror (SSM); there is a small degree of polarization in the IR for uncoated gold mirrors
- The orientation of the polarization axis of the scene select mirror changes with scene mirror rotation.
- When coupled with the polarization sensitivity of the sensor, this produces a radiometric modulation of the detected signal that is dependent on the rotation angle of the scene select mirror and creates a calibration error.

CrIS Calibration Bias due to Polarization. Current Model:

- For CrIS the bias due to ignoring polarization can be approximated as:

$$E_p \cong p_r p_t \left\{ \left(L_S - B_{SSM} \right) \left[\cos 2\left(\delta_S - \alpha \right) + \cos 2\alpha \right] \right\}$$

  where p_r and p_t are the SSM and sensor polarizations, L_s is the scene radiance, B_{SSM} is $B(T_{SSM})$, δ_s is the scene mirror angle, and α is the sensor axis orientation angle.
- Currently using spectrally independent values for scene mirror polarization and sensor polarization: p_r = 0.0055, p_t = 0.08 (average values provided by Joe Predina)
- Selected nadir view as 0° for α and δ
- Have assumed that sensor polarization orientation is dominated by the beamsplitter (α = 0°). The impact of other optical elements need to be evaluated (dichroics in particular).
- Will revise model as better information becomes available, but these preliminary values allow us to demonstrate the nature and potential calibration bias due to uncorrected polarization.

CrIS Calibration Bias due to Polarization. Current Model:

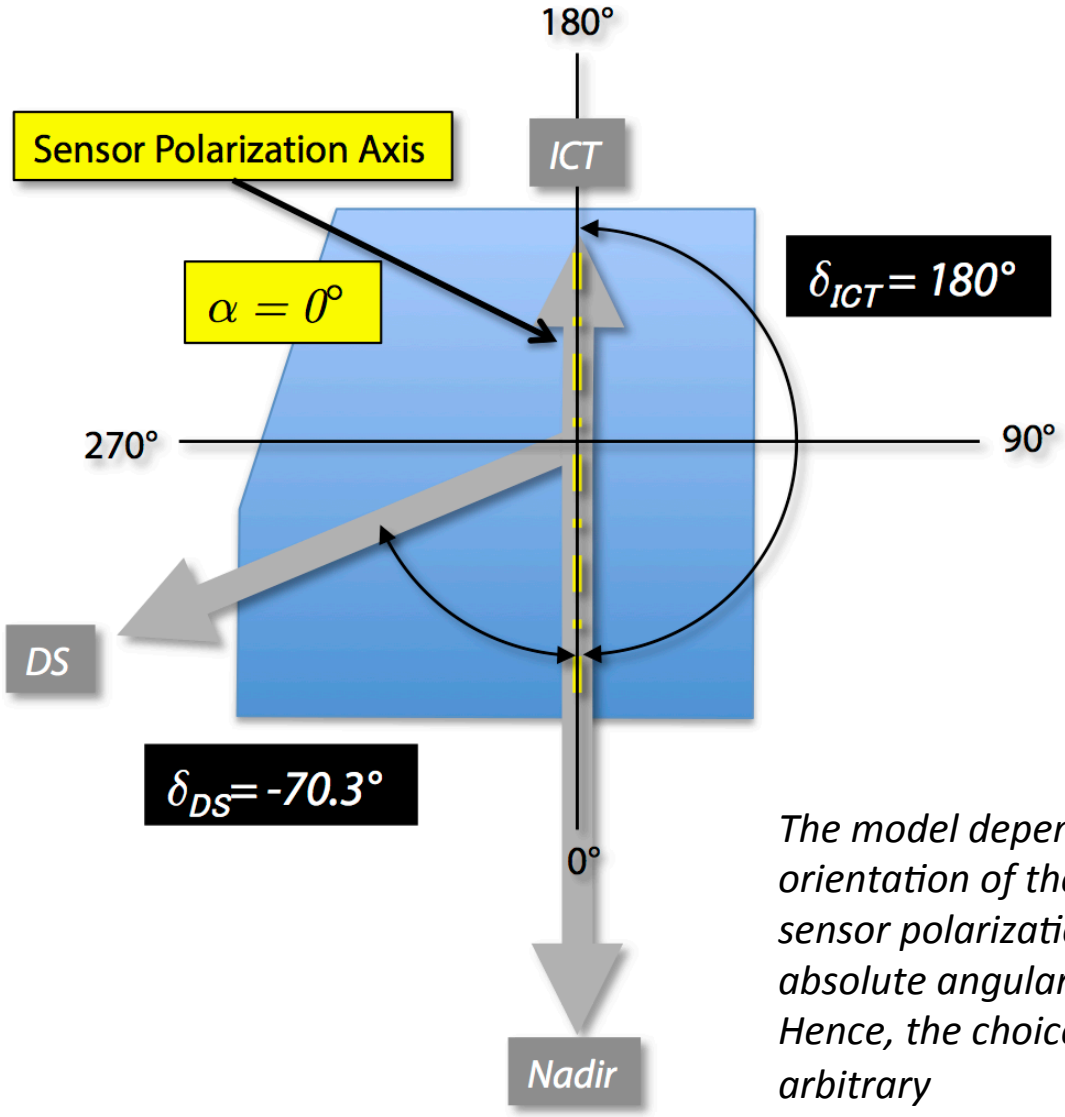

The model depends on the relative orientation of the scene mirror and sensor polarization axes, not the absolute angular position of either. Hence, the choice of the 0° position is arbitrary

CrIS Calibration Bias due to Polarization. Model Results at 900 cm^{-1}

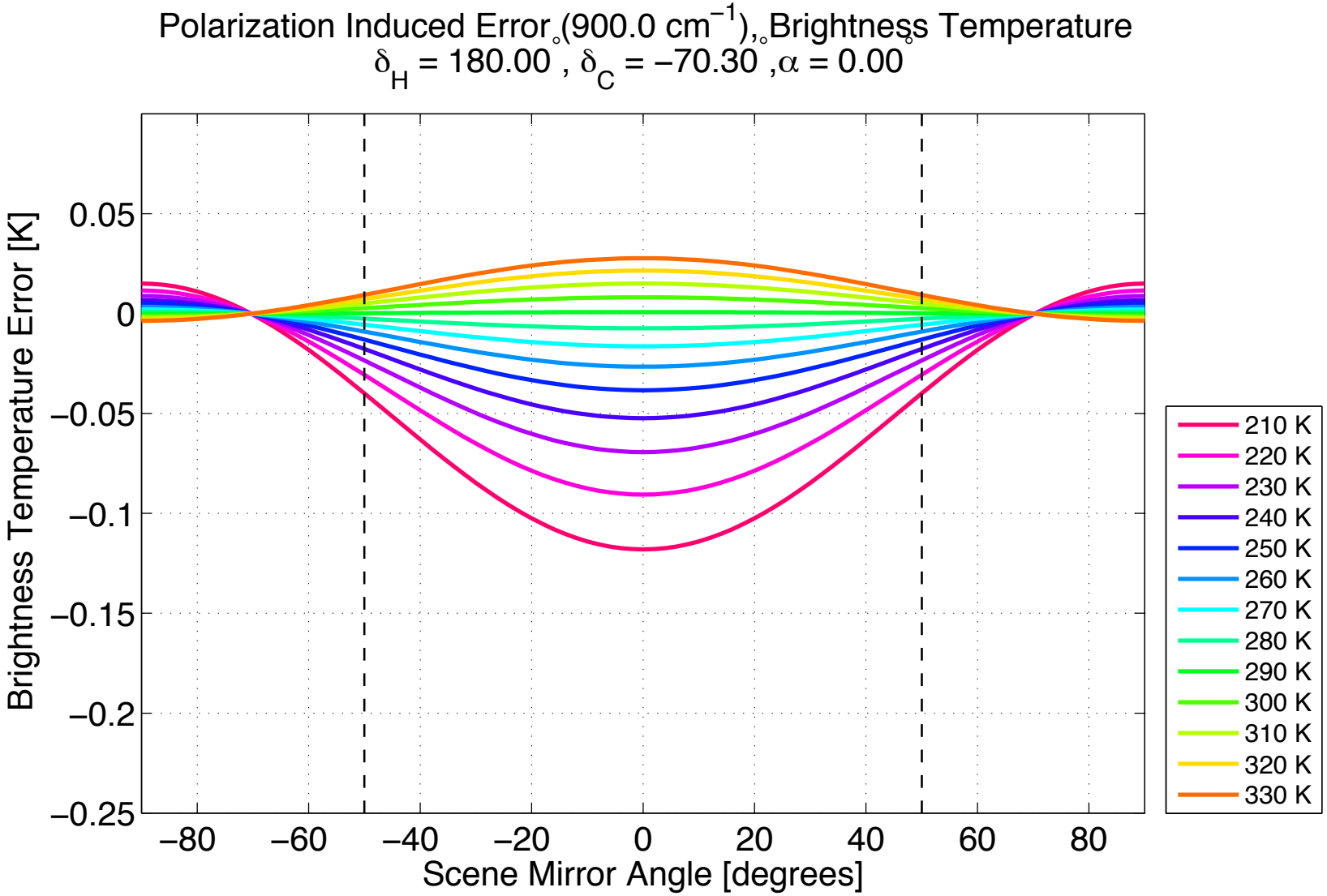

CrIS Calibration Bias due to Polarization.
Band 15 CrIS/VIIRS comparisons and 11 μm Model Results

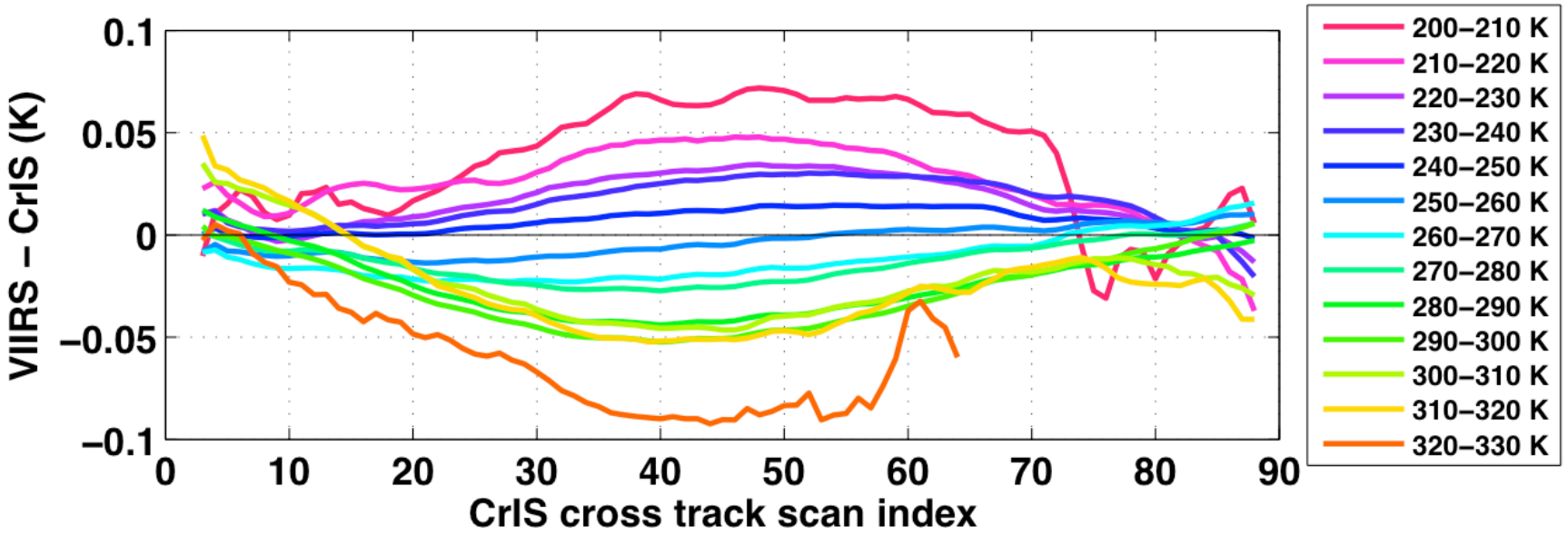

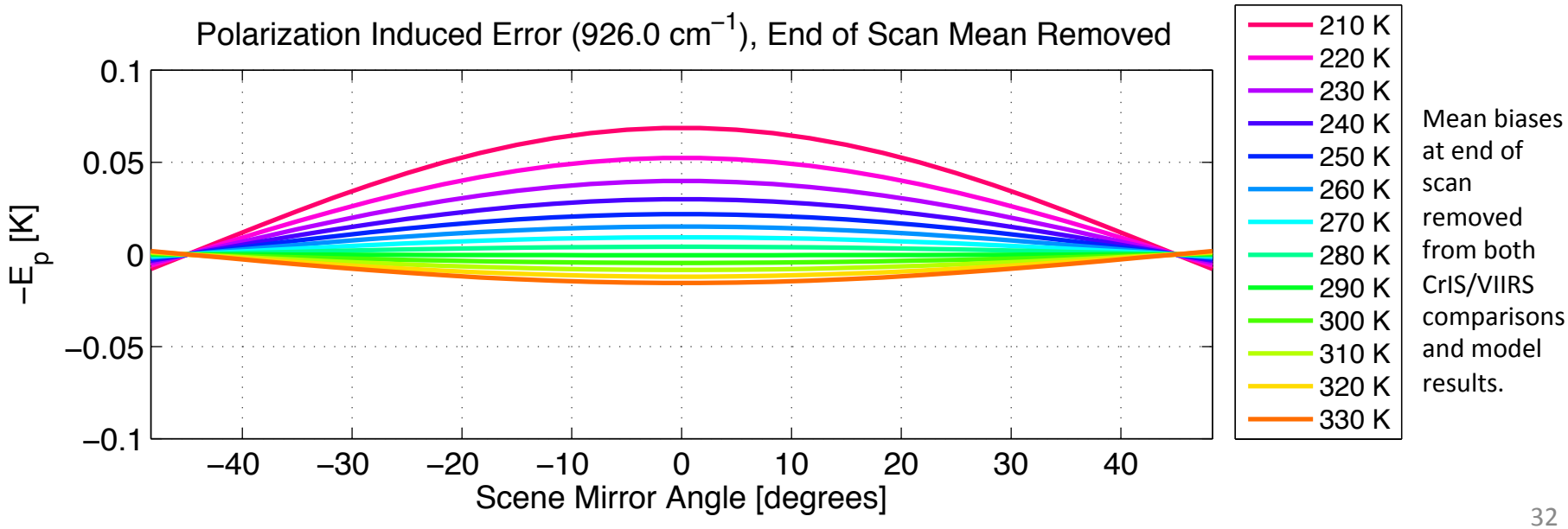

Mean biases at end of scan removed from both CrIS/VIIRS comparisons and model results.

CrIS Calibration Bias due to Polarization. Model Results at nadir (FOR15)

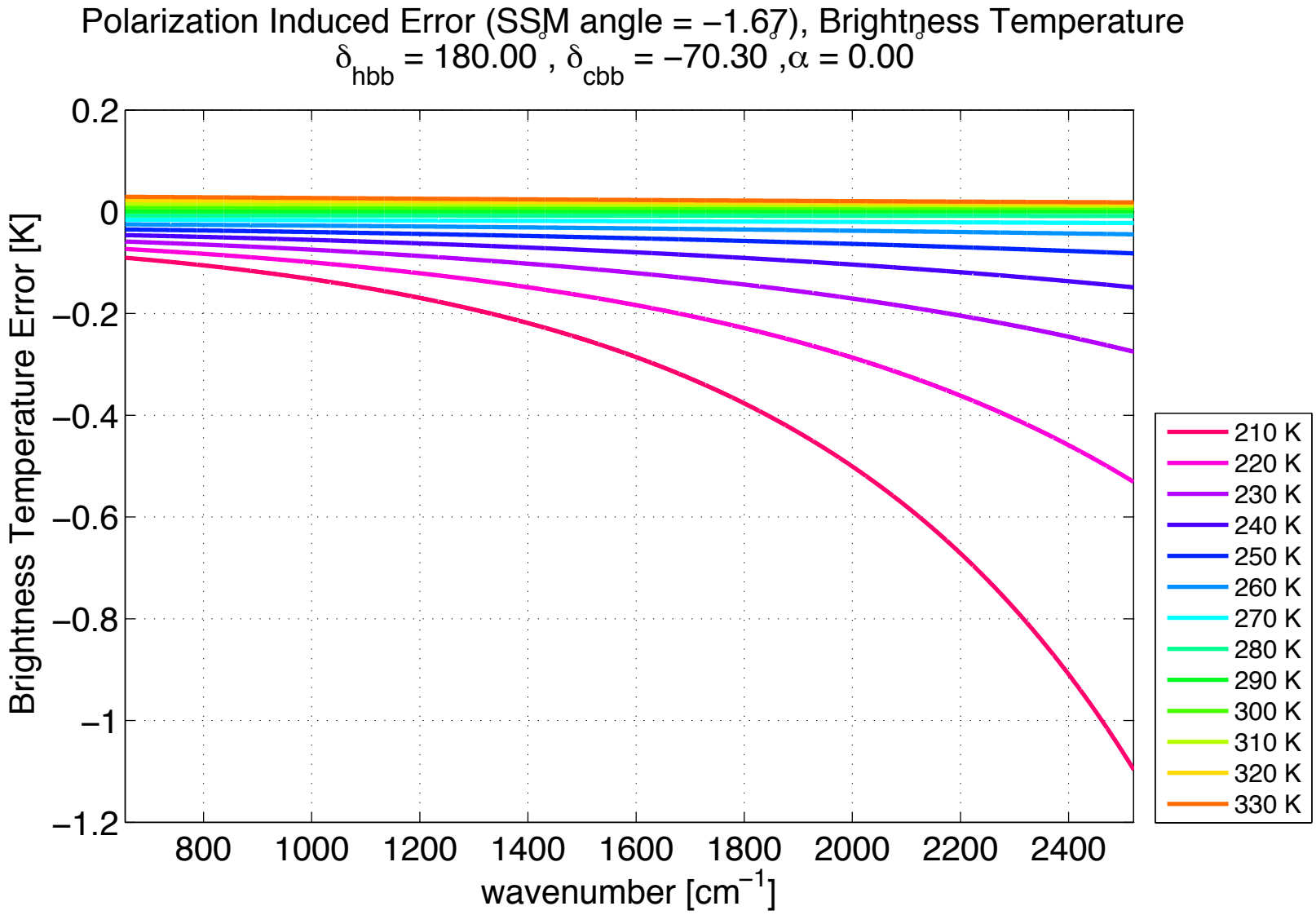

CrIS Calibration Bias due to Polarization. Summary

- **Current CrIS Calibration does not account for polarization effects.**
- **However, we should expect systematic effects due to the design of the sensor and there is evidence of the effects in observed spectra.**
- **A correction module suitable for use in the SDR algorithm is being developed.**
- **Additional measurements of key optical components should be performed to ensure accurate corrections.**

J1 CrIS Radiometric Calibration: Overall Summary

- **J1 CrIS pre-launch calibration uncertainty is dominated by ICT temperature knowledge (114 mK) and quadratic nonlinearity coefficient uncertainty (~25%).**
- **Radiometric Uncertainty estimates for TVAC ECT views are less than ~0.3 K. After nonlinearity tuning, differences between CrIS calibrated spectra and predicted ECT view spectra are less than ~0.1 K for scene temperatures of 233K-310K.**
- **Using pre-launch parameters and uncertainties, RU for example Earth view spectra has been estimated. With the exception of FOVs with largest nonlinearity (LW5 and MW9), RU is less than a few tenths K.**
- **CrIS has systematic biases due to Polarization which varies with scan angle, scene temperature, and wavelength, and associated correction modules are being developed for consideration in the SDR algorithm.**

J1 CrIS Radiometric Calibration: Future Work

- **The ICT temperature knowledge uncertainty (114 mK) includes a large contribution (~75 mK) due to the estimated gradient from the PRTs to the emitting surface; We plan to investigate this further and possibly account for part of the gradient in the effective ICT temperature and reduce its uncertainty.**
- **Pending results of NIST TXR measurements of the ECT, we may re-visit our nonlinearity analysis.**
- **After launch, nonlinearity coefficients will be fine-tuned to create optimal consistency among MW FOVs and LW FOVs for Earth view data, using the most linear FOVs/detectors as reference. This should reduce the uncertainty for FOVs with largest nonlinearity including LW5 and MW9.**
- **Pursue additional polarization measurements and study the impact of polarization corrections on Earth view spectra, including near-nadir comparisons with other sensors via SNOs, and the impact on cold scene SW band calibration.**

Summary Continued:
J1 CrIS is as good or better than S-NPP CrIS

- **J1 ICT emissivity is higher and well characterized**
- **ICT temperature uncertainties similar**
- **Nonlinearity:**
  - **LW: overall a2 magnitudes are similar but J1 and S-NPP have different FOV dependence.**
  - **MW: 8 of 9 detectors on J1 are very linear.**
- **Both expected to have similar polarization effects**

Other Work

- **S-NPP LW FOV5 cold scene anomaly**
- **S-NPP SW cold scene biases**
- **Correction for on-board non-circular FIR filtering (spectral ringing, extended interferograms)**
- **Choice of Calibration Equation (spectral ringing)**